Neuro-Oncology

20(8), 1044–1054, 2018 | doi:10.1093/neuonc/noy028 | Advance Access date 23 February 2018

Sprouty2 enhances the tumorigenic potential of glioblastoma cells

Jong-Whi Park, Guido Wollmann, Carles Urbiola, Barbara Fogli, Tullio Florio, Stephan Geley, and Lars Klimaschewski

Division of Neuroanatomy, Medical University of Innsbruck, Innsbruck, Austria (J.-W.P., B.F., L.K.); Christian Doppler Laboratory for Viral Immunotherapy of Cancer, Division of Virology, Medical University of Innsbruck, Innsbruck, Austria (G.W., C.U.); Section of Pharmacology, Department of Internal Medicine and Center of Excellence for Biomedical Research, University of Genova, Genova, Italy (T.F.); Division of Molecular Pathophysiology, Medical University of Innsbruck, Innsbruck, Austria (S.G.)

Corresponding Authors: Stephan Geley, Medical University of Innsbruck, Innrain 80–82, 6020 Innsbruck, Austria (stephan.geley@i-med.ac.at); Lars Klimaschewski, Medical University of Innsbruck, Muellerstrasse 59, 6020 Innsbruck, Austria (lars.klimaschewski@i-med.ac.at).

Abstract

Background. Sprouty2 (SPRY2), a feedback regulator of receptor tyrosine kinase (RTK) signaling, has been shown to be associated with drug resistance and cell proliferation in glioblastoma (GBM), but the underlying mechanisms are still poorly defined.

Methods. *SPRY2* expression and survival patterns of patients with gliomas were analyzed using publicly available databases. Effects of RNA interference targeting SPRY2 on cellular proliferation in established GBM or patient-derived GBM stemlike cells were examined. Loss- or gain-of-function of SPRY2 to regulate the tumorigenic capacity was assessed in both intracranial and subcutaneous xenografts.

Results. SPRY2 was found to be upregulated in GBM, which correlated with reduced survival in GBM patients. SPRY2 knockdown significantly impaired proliferation of GBM cells but not of normal astrocytes. Silencing of SPRY2 increased epidermal growth factor-induced extracellular signal-regulated kinase (ERK) and Akt activation causing premature onset of DNA replication, increased DNA damage, and impaired proliferation, suggesting that SPRY2 suppresses DNA replication stress. Abrogating SPRY2 function strongly inhibited intracranial tumor growth and led to significantly prolonged survival of U87 xenograft-bearing mice. In contrast, SPRY2 overexpression promoted tumor propagation of low-tumorigenic U251 cells.

Conclusions. The present study highlights an antitumoral effect of SPRY2 inhibition that is based on excessive activation of ERK signaling and DNA damage response, resulting in reduced cell proliferation and increased cytotoxicity, proposing SPRY2 as a promising pharmacological target in GBM patients.

Keywords

DNA damage response | ERK | glioblastoma | Sprouty2 | replication stress

Glioblastoma (GBM) is a malignant brain tumor[1] with a median survival of approximately 15 months and poor responses to current therapeutic approaches.[2,3] Single-cell RNA sequencing showed that individual tumors are composed of multiple molecular subtypes (classical, mesenchymal, proneural, and neural subtypes), suggesting intratumor heterogeneity.[4] Thus, a better understanding of the underlying molecular mechanisms that define tumor cell populations is crucial and may improve GBM therapy.

Large-scale molecular studies have identified key genetic alterations that may contribute to the development of GBM. Alterations in receptor tyrosine kinase (RTK)-mediated signaling pathways have been reported to occur in 88% of GBM.[5] As a regulator of RTK signaling, Sprouty

Importance of the study

As a regulator of RTK signaling, SPRY2 is essential for GBM cell proliferation and tumorigenicity. As a consequence of hyperactivation of ERK signaling, the inhibitory effect on cell proliferation by silencing of SPRY2 is specific to GBM but not to normal astrocytes, suggesting that GBM cells are strongly addicted to elevated SPRY2 expression. Low *SPRY2* expression is associated with better prognosis in malignant glioma patients, suggesting that modulation of SPRY2 may provide a novel avenue for GBM therapies.

(SPRY) protein was first identified in *Drosophila*,[6,7] and 4 SPRY (SPRY1–4) proteins have been described in mammals.[8] Among these 4 isoforms, SPRY2 reveals the highest sequence homology across species.[8] In most cancers, SPRY2 has been shown to be dysregulated, but the effects of SPRY2 on malignancy strongly depend on cancer type.[9] Tumor suppressive roles of SPRY2 are well established in breast, liver, lung, and prostate cancers,[10–13] while in colon cancer, in which SPRY2 is highly expressed in undifferentiated high-grade tumors[14] and enhances proliferation and metastasis,[15] SPRY2 acts like an oncogene.

In GBM, the function of SPRY2 is not well understood. An earlier study showed that SPRY2 protein levels are significantly decreased in about 80% of human gliomas (World Health Organization grades II–IV), implying a putative tumor suppressing function.[16] Conversely, SPRY2 knockdown (KD) has been demonstrated to potentiate responses to RTK inhibitors and decrease proliferation in GBM cells.[17] More recently, transcriptome analysis revealed that gliomas with high expression of *SPRY* isoforms (SPRY1, -2, and -4) and low expression of neurofibromin 1 (*NF1*) and phosphatase and tensin homolog (*PTEN*) are associated with poor prognosis compared with tumors with a reversed expression pattern.[18] Here, we provide evidence that SPRY2 inhibition confers high extracellular signal-regulated kinase (ERK) activity and sensitizes GBM cells to DNA damage response, leading to decreased cell proliferation and reduced tumorigenicity.

Materials and Methods

Cell Lines and Cell Culture

Patient-derived primary GBM stemlike cells were obtained from IRCCS-AOU San Martino-IST (Genova, Italy).[19] Cells were grown in serum-free medium (Dulbecco's modified Eagle's medium [DMEM]-F12/Neurobasal [1:1] with 1% B27 [Thermo Fisher Scientific], 2 mM L-glutamine [Gibco] and supplemented with 20 ng/mL each of epidermal growth factor [EGF; Sigma] and fibroblast growth factor 2 [FGF2; provided by Dr P. Claus, Hannover]). Cells were cultured as monolayer on Matrigel (Corning). The standard GBM cell lines U87, T98G, U251, U118, U1242, and SF126 (provided by Dr M. Reindl, Innsbruck) were cultured in DMEM (Sigma) with 10% fetal bovine serum (FBS; Gibco), 1% antibiotic-antimycotic (ABAM; Gibco), and 2 mM L-glutamine (Gibco). Human astrocytes (ScienCell) were maintained in the recommended medium (ScienCell) supplemented with 2% FBS, 100 units/mL penicillin, and 100 µg/mL streptomycin. All cells were grown in 5% CO_2 humidified incubator at 37 °C. U87, T98G, and U251 cell lines were authenticated by short tandem repeat analysis (Microsynth) within the past 12 months.

Plasmids and Reagents

For short hairpin (sh)RNA-mediated depletion, annealed oligonucleotide targeting SPRY2 (shRNA target: GCAGGTACATGTCTTGTCT) was inserted into pGLTR-puro plasmid for a stable and conditional RNA interference (RNAi) system.[20] As a control, shRNA targeting luciferase was used. For stable transgene expression, lentiviral plasmids encoding VNP (Venus-NLS-PEST) or N-terminal, Flag-tagged SPRY2 were cloned. $SPRY2^{S121A}$ mutant, RNAi-resistant-SPRY2, or -luciferase were generated using site-directed mutagenesis. The mitogen-activated protein kinase kinase (MEK) inhibitor PD98059 (Sigma) was used to inhibit ERK activity.

Establishment of Stable Cell Lines

Lentiviral particles were produced by co-transfection of human embryonic kidney 293T cells with the lentiviral plasmids as well as helper plasmids psPAX2 and VSV-G. Culture media were harvested after 48 hours of transfection and further used for infection with 4 µg/mL polybrene (Sigma). Target cells were infected with 0.2 µm filtered lentivirus for 24 hours and cells expressing the respective transgene were selected using 2 µg/mL puromycin (Sigma). For stable expression of RNAi-insensitive-SPRY2 or -firefly luciferase, retroviral transduction was performed by transfection of Phoenix cells with pQCXIN plasmid encoding the transgene, and transduced cells were selected with 500 µg/mL G418 (Sigma). After transduction, transgene expression was analyzed by reverse transcription quantitative (RT-q) PCR. Detailed experimental procedures for RT-qPCR and immunostaining are described in the Supplementary Methods.

Immunoblotting

Total cell lysates were prepared followed by boiling and sonication. Equal amounts of proteins were separated by sodium dodecyl sulfate-polyacrylamide gel electrophoresis, transferred to nitrocellulose membrane (GE Healthcare). Membranes were blocked with 10% low fat skim milk (Marvel) and 0.5% nonyl phenoxypolyethoxylethanol (NP40) in phosphate buffered saline (PBS), and incubated

with primary antibodies: anti-SPRY2 (Abcam, 1:1000), anti-α-tubulin (TAT1, 1:10000), anti-pERK (Cell Signaling Technology, 1:1000), anti-ERK (Cell Signaling Technology, 1:1000), anti-pAkt (Cell Signaling Technology, 1:1000), anti-Akt (Cell Signaling Technology, 1:1000), anti-poly(ADP-ribose) polymerase (PARP) (Cell Signaling Technology, 1:1000), and anti-γH2AX (Cell Signaling Technology, 1:1000). Bound antibodies were detected using goat anti-mouse or anti-rabbit horseradish peroxidase-linked secondary antibodies (Dako) and enhanced chemiluminescence reagent (Thermo Fisher Scientific).

Cell Growth Measurement and Cell Cycle Analysis

For measuring cellular proliferation, cells were seeded at 100000 cells per well in 6-well plates and counted using a hemocytometer 4 days later. The values of doubling times were obtained applying the exponential growth formula and further used for calculation of doublings per day as previously reported.[21] To measure cytotoxicity, trypan blue (Sigma)-positive cells were counted. For cell cycle analysis, cells were harvested and fixed with 70% ethanol overnight at 4°C. The following day the cells were washed twice with PBS and incubated with 40 μg/mL propidium iodide solution (Sigma) containing 100 μg/mL RNase A (Promega) for 30 minutes at 37°C. The cell cycle phase was determined by flow cytometry (LSR-Fortessa, BD Biosystems) and analyzed using FlowJo software.

GBM Xenograft Models

Six- to 8-week-old female Naval Medical Research Institute nu/nu mice were purchased from Janvier Labs. Mice were anesthetized with ketamine/xylazine and stereotactically implanted with U87 (5×10^5) or U251 (1×10^6) cells in 5 μL PBS into the right striatum. Bioluminescence imaging was performed using the Lumina In Vivo Imaging System (PerkinElmer), as reported.[22] Mice were sacrificed when animals showed more than 20% weight loss or neurological symptoms. Subcutaneous cell injection was performed with U87 (2×10^6) or U251 (1.5×10^6) cells in 100 μL PBS. The width and length of subcutaneous tumor xenografts were measured every 4 to 5 days using a caliper. The tumor volume in cubic millimeters was calculated as width^2 × length × 0.4. Mice were euthanized when the tumor volume exceeded 800 mm^3. At the end of the study, subcutaneous tumors were excised for immunohistochemical analysis of Ki67. For inducible silencing of SPRY2, 0.5 mg/mL of doxycycline (Sigma) for subcutaneous implantation or 1 mg/mL of doxycycline for intracranial implantation with 5% sucrose (Sigma) was freshly administered every 4–7 days into drinking water. All animal experiments were performed with the approval of the institutional review board and the Austrian Federal Ministry of Science (BMWFW-66.011/0041-WF/V/3b/2016).

Analysis of SPRY2 mRNA Expression and Patient Survival

The expression of *SPRY* isoforms in The Cancer Genome Atlas (TCGA) GBM[5] GSE7696[23] and GSE36245[24] datasets was examined using the R2 genomics analysis and visualization platform (http://r2.amc.nl). For comparison with nontumor, lower-grade glioma or other cancer tissues, *SPRY2* expression in TCGA and GSE4290[25] datasets was analyzed using ONCOMINE[26] or The Cancer Immunome Atlas (https://tcia.at/home). The GlioVis data portal for visualization and analysis of brain tumor expression datasets[27] was used for the patient survival analysis within TCGA[5,28] datasets.

Statistical Analysis

All experiments are represented as mean ± SEM or SD and analyzed using GraphPad Prism software version 7.0. For significance calculation, unpaired *t*-test or one-way ANOVA was used to compare differences between 2 independent groups or among multiple independent groups, respectively. The statistical significance is indicated as $*P < 0.05$, $**P < 0.01$, and $***P < 0.001$.

Results

Upregulation of SPRY2 Correlates with Reduced Overall Survival in GBM Patients

Sprouty genes (*SPRY*1–4), together with *PTEN* and *NF1*, are used as molecular signatures for clustering adult diffuse gliomas.[18] To investigate which SPRY isoforms correlate with the malignancy of GBM, we first compared the mRNA expression of 4 different *SPRY* isoforms in GBM using the R2 genomics analysis and visualization platform. Analysis of all 3 GBM microarray gene expression profiles[5,23,24] demonstrated that among the *SPRY* genes, *SPRY2* was strongly expressed in GBM (Fig. 1A). In large transcriptome datasets, we next compared *SPRY2* mRNA expression levels in 19 different cancers and corresponding normal tissues. GBM expressed the highest levels of *SPRY2* among different cancers (Supplementary Fig. S1A). Moreover, its expression in GBM was found to be significantly higher than that in normal brain tissues (Fig. 1B and Supplementary Fig. S1A). *SPRY2* expression correlated positively with glioma grade in the dataset of TCGA[28] (Supplementary Fig. S1B). We further tested the above findings in culture, using normal human astrocytes, an established GBM cell line (U87), as well as patient-derived GBM stem cells (GSCs) maintained in the absence of serum. SPRY2 expression in human astrocytes and GSC1 was relatively modest, whereas U87 and GSC2 expressed high levels of SPRY2 (Fig. 1C). *SPRY2* mRNA expression correlated well with protein levels in GBM-derived cell lines ($R^2 = 0.615$; Supplementary Fig. S1C, D).

Because the above data suggested a strong correlation between *SPRY2* expression levels and malignancy, we next examined whether there was any correlation between *SPRY2* expression and survival of glioma patients. As reported previously,[17] the Kaplan–Meier plot indicates that GBM[5] patients with low mRNA expression of *SPRY2* had a significantly better clinical outcome ($P < 0.001$; Fig. 1D). Intriguingly, low expression of *SPRY2* is associated with prolonged overall survival in glioma patients,[28] regardless of isocitrate dehydrogenase mutation status (Supplementary Fig. S2).

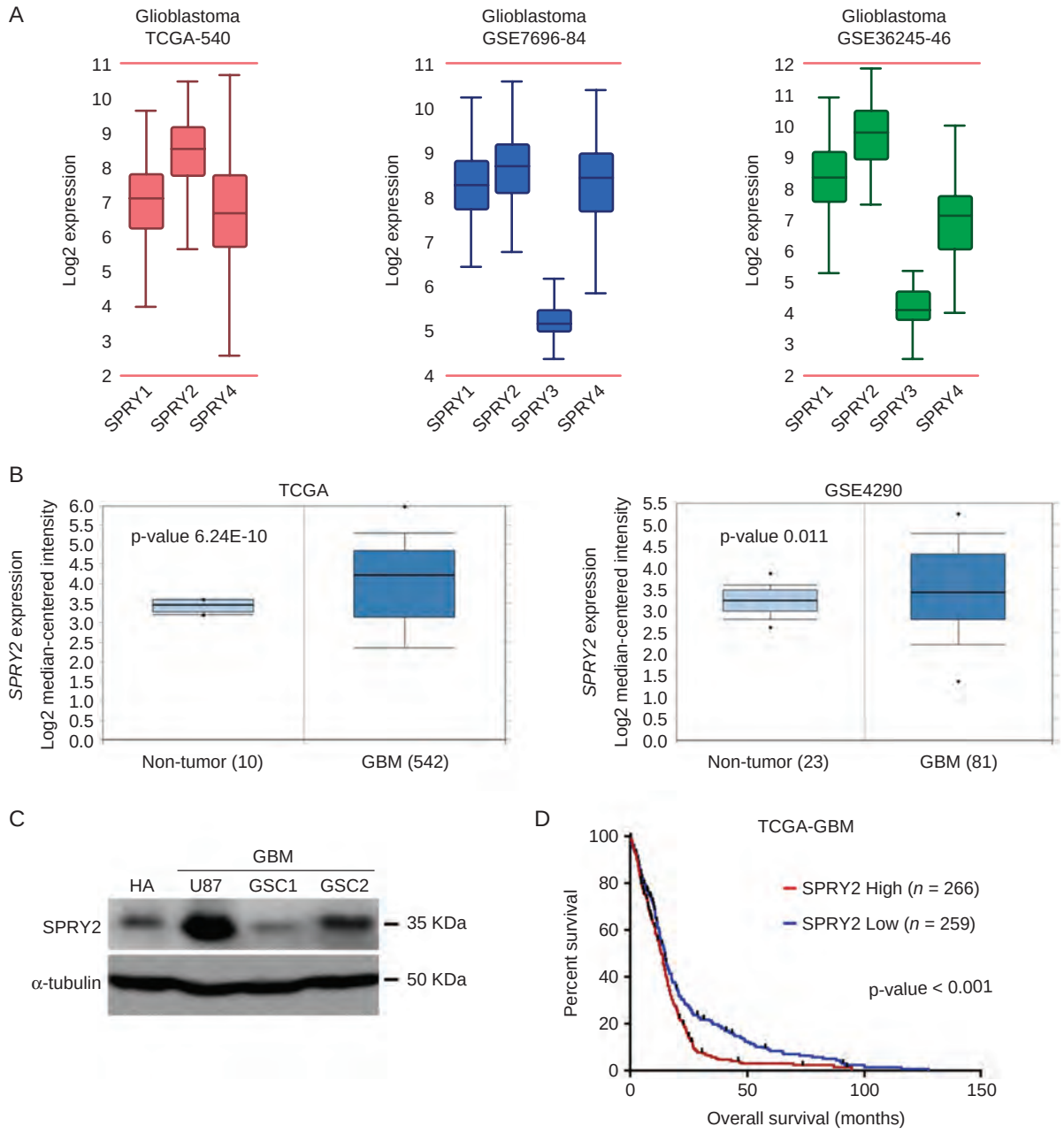

Fig. 1 SPRY2 is strongly expressed in GBM and its expression correlates with reduced overall survival in GBM patients. (A) The mRNA expression of 4 different SPRYs (*SPRY1-4*) in 3 GBM datasets using the R2 genomics analysis and visualization platform (http://r2.amc.nl). (B) *SPRY2* expression levels in GBM compared with that of nontumor samples. TCGA and GSE4290 datasets, including *P*-values, were analyzed using ONCOMINE. (C) Levels of endogenous SPRY2 protein in normal human astrocyte (HA), U87 and GBM stemlike cells (GSC1 and GSC2) as determined by immunoblot. (D) Overall survival differences among GBM patients are shown as Kaplan–Meier survival curve with high and low mRNA expression of *SPRY2* from TCGA dataset. ***$P < 0.001$ by the log-rank test.

Inhibition of Cell Proliferation by Downregulation of SPRY2 Is GBM-specific

To understand the role of SPRY2 in GBM biology, we transduced U87 cells with lentiviral vectors for doxycycline (Doxy)-inducible shRNA expression for SPRY2 KD (Fig. 2A) or luciferase as a control (Supplementary Fig. S3A). Because long-term serum-cultured GBM cell lines can differ in several aspects from primary GBM cells,[29] we also utilized primary cells (GSC1 and GSC2) from GBM patients to increase the clinical relevance of this analysis (Fig. 2B). Cell proliferation was significantly reduced in SPRY2 KD cell cultures but not in cells expressing shRNA targeting luciferase (Fig. 2C, D). Upon reconstitution of SPRY2

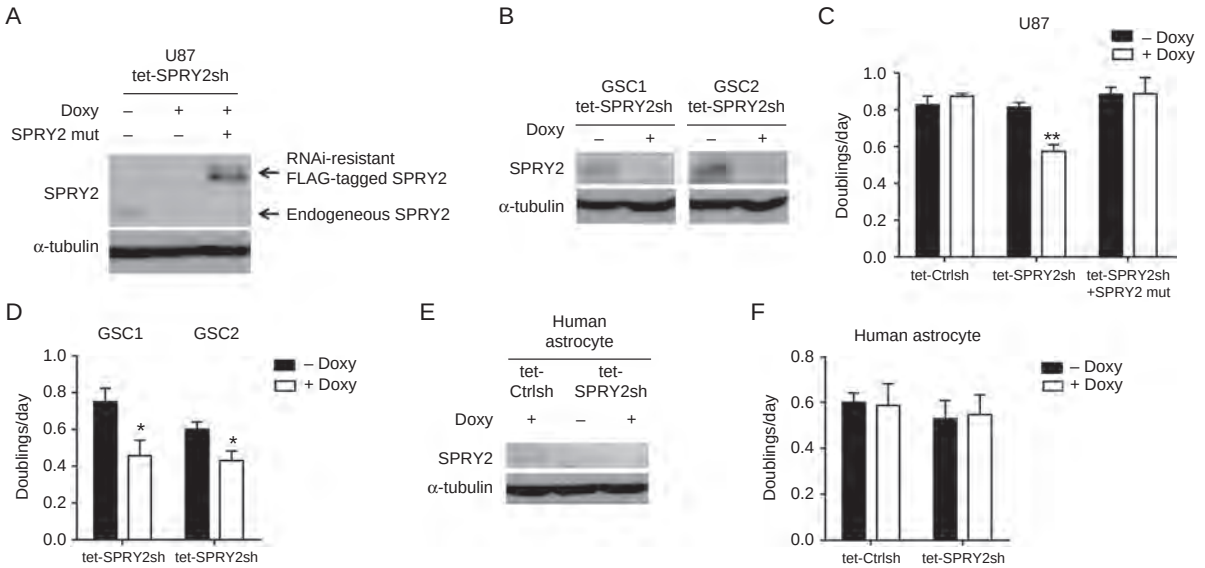

Fig. 2 SPRY2 suppression inhibits cell proliferation of GBM but not of normal human astrocytes. (A and B) U87, GSC1, or GSC2 cells expressing doxycycline-inducible SPRY2-shRNA were treated with or without 1 μg/mL doxycycline for 72 hours, and SPRY2 protein levels were determined by immunoblot. For reconstitution of SPRY2 expression in U87 tet-SPRY2sh cells, RNAi-resistant Flag-tagged SPRY2 was used. (C and D) Doublings per day of U87, GSC1, or GSC2 transduced with luciferase-shRNA (tet-Ctrlsh) or tet-SPRY2sh as assessed by cell counting. (E) Human astrocytes transduced with tet-Ctrlsh or tet-SPRY2sh were treated with or without 1 μg/mL doxycycline for 72 hours, and SPRY2 protein levels were assessed by immunoblot. (F) Measurement of human astrocyte proliferation as doublings per day. Mean ± SEM of at least 3 independent experiments. $*P < 0.05$, $**P < 0.01$.

expression by retrovirus-mediated transduction of an RNAi-resistant version of SPRY2 in U87 tet-SPRY2sh cells, this proliferation defect could be restored, proving the specificity of the SPRY2-RNAi effect (Fig. 2A, C). Along with the inhibition of cell proliferation, a cytotoxic effect was also observed in U87 and GSC1 SPRY2 KD cells (Supplementary Fig. S3B, C). Thus, increased cell death as well as reduced generation time may both contribute to impaired proliferation. To determine whether knockdown of SPRY2 would also affect the proliferation of primary nontransformed cells, we also transduced normal human astrocytes for loss-of-function experiments (Fig. 2E). Intriguingly, silencing of SPRY2 had no effect on the proliferative capacity of human astrocytes (Fig. 2F), suggesting that SPRY2 might exert a GBM-specific activity.

Impaired Proliferation in SPRY2 KD Cells Depends on ERK Signaling

SPRY2 protein negatively regulates RTK-dependent signaling in response to growth factors.[30,31] To test the canonical function of SPRY2 in U87 and GSC1 cells, we examined signaling downstream of EGF receptor activation in induced and non-induced SPRY2 KD cells. In response to EGF treatment, downregulation of SPRY2 resulted in a strong increase and prolonged duration of ERK activation in both U87 and GSC1 cells (Fig. 3A). Similarly, Akt was also more strongly activated in SPRY2 KD cells than in controls. Interestingly, during EGF stimulation, SPRY2 levels in GSC1 cells increased to levels similar to the basal expression levels of U87 cells (Fig. 3A). This suggests that in GSC1 cells, SPRY2 expression is still embedded in the negative feedback regulation loop downstream of RTK activation, while in U87 cells SPRY2 is constitutively expressed, which may be a result of the continued growth in high serum conditions, consistent with its function as a negative regulator of RTK signaling.

To investigate whether the consequence of SPRY2 KD on cell proliferation is dependent on hyperactivation of the ERK signaling pathway, we used the MEK inhibitor PD98059 (MEKi), which attenuated ERK activity in a dose-dependent manner (Fig. 3B). Importantly, treatment of PD98059 reversed the inhibitory effect on cell proliferation of SPRY2 KD (Fig. 3C), indicating that high ERK activity is required for SPRY2 KD-induced impaired proliferation.

Silencing of SPRY2 Causes Premature S-phase Entry and DNA Damage

The above experiment confirmed that SPRY2 is functionally intact in both U87 and GSC1 cells, and exerts its canonical function as an inhibitor of mitogenic ERK activation. Despite this effect, however, silencing of SPRY2 reduced proliferation of GBM cells (Fig. 2). As oncogene-induced DNA replication stress results in DNA damage-induced cell cycle arrest, senescence, or apoptosis,[32] we hypothesized that increased ERK activation due to knockdown of SPRY2 in growth

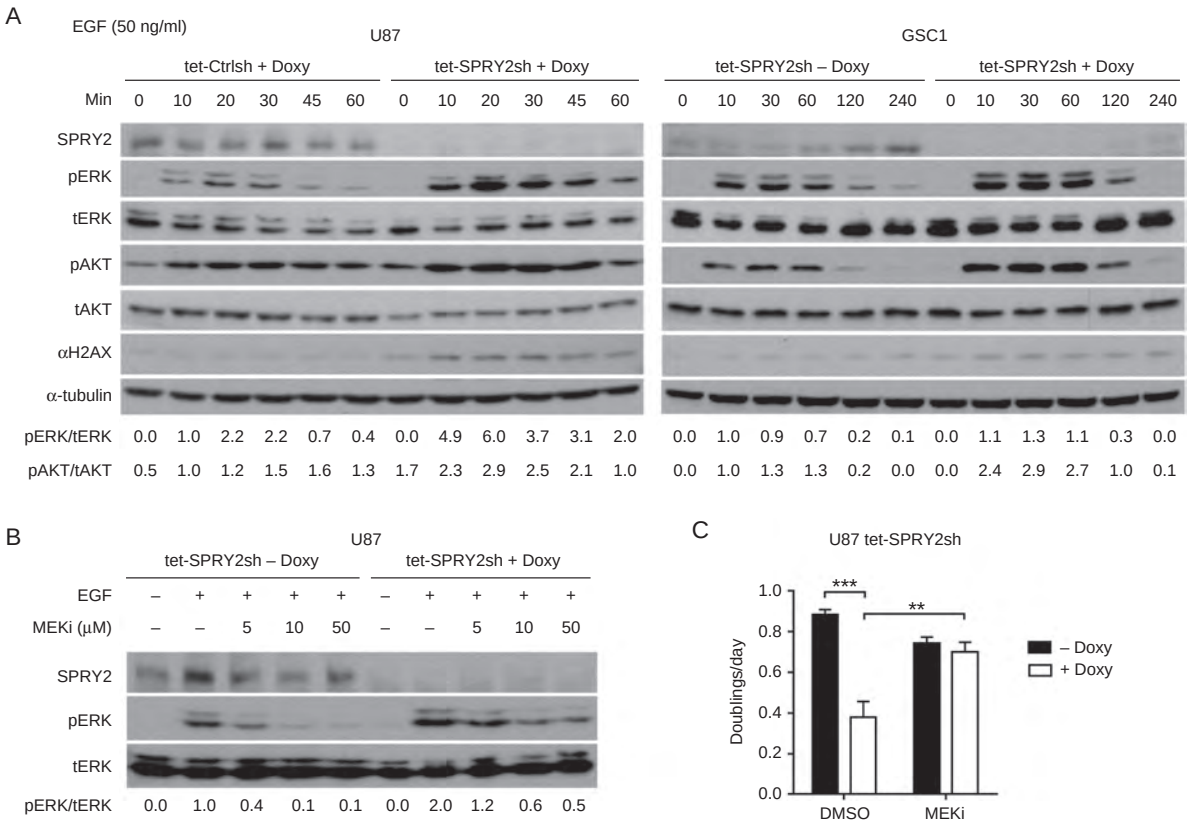

Fig. 3 Silencing of SPRY2 increases ERK and Akt activation, and MEK inhibitor prevents the decreased cell proliferation of SPRY2 KD. (A) U87 or GSC1 cells transduced with tet-Ctrlsh or tet-SPRY2sh were treated with or without 1 μg/mL doxycycline for 72 hours, serum- (U87) or EGF and FGF2- (GSC1) starved overnight, then treated with EGF (50 ng/mL) for the indicated times. Immunoblotting was performed with the indicated antibodies. (B) Immunoblots for the indicated proteins in U87 tet-SPRY2sh cells (± Doxy) pretreated with the indicated concentrations of PD98059 or dimethyl sulfoxide (DMSO), and stimulated with EGF (20 ng/mL) for 20 minutes. (C) Measurement of cell proliferation of U87 tet-SPRY2sh cells (± Doxy) in the presence of DMSO or 10 μM PD98059. Mean ± SEM of at least 3 independent experiments. $^{**}P < 0.01$, $^{***}P < 0.001$.

promoting conditions may also result in premature entry into S-phase and DNA replication stress. To examine whether SPRY2 KD accelerated cell cycle progression into S-phase, we performed bromodeoxyuridine (BrdU) incorporation assays in induced and non-induced SPRY2 KD cells. As can be seen in Fig. 4A, the number of BrdU-positive cells was significantly increased in SPRY2 KD cells 4 hours after EGF stimulation. Furthermore, we performed immunoblotting and immunostaining with a marker for DNA damage to test whether SPRY2 KD induces DNA replication stress. As expected, phosphorylated H2AX (γH2AX), a marker for double-strand DNA breaks, was markedly increased in U87 and GSC1 SPRY2 KD cells (Figs. 3A and 4B, C). In addition, SPRY2 KD induced PARP cleavage, indicating the induction of apoptotic cell death (Fig. 4C). Thus, the reduced proliferation upon depletion of SPRY2 might be due to DNA replication stress triggered by oncogenic activity (eg, the activation of the Ras-Raf-mitogen-activated protein kinase [MAPK] cascade in GBM).

Conditional Knockdown of SPRY2 Inhibits GBM Tumor Growth

To assess whether RNAi targeting SPRY2 exerts antitumoral effects in vivo, we next performed intracranial implantation of U87 cells stably expressing a luciferase variant resistant to RNAi in female athymic mice (n = 5/group). Three days before tumor implantation, oral doxycycline treatment was initiated. Intracranial xenografts were then generated in Doxy-treated mice by implantation of Doxy-inducible SPRY2-shRNA cells. As a control, Ctrl-shRNA cells were also used to exclude nonspecific effects of doxycycline treatment on tumor growth. Bioluminescence imaging showed the inhibited tumor growth in Doxy-treated tet-SPRY2sh tumor-bearing mice compared with control mice (Fig. 5A). Strikingly, bioluminescence signal was not present in Doxy-treated tet-SPRY2sh mice (4/5) over 9 weeks, which translated into a prolonged survival of mice (P = 0.002; Fig. 5B). In contrast, Doxy-treated tet-Ctrlsh tumors grew substantially, reaching the clinical endpoint (median survival 27 days) (Fig. 5A,

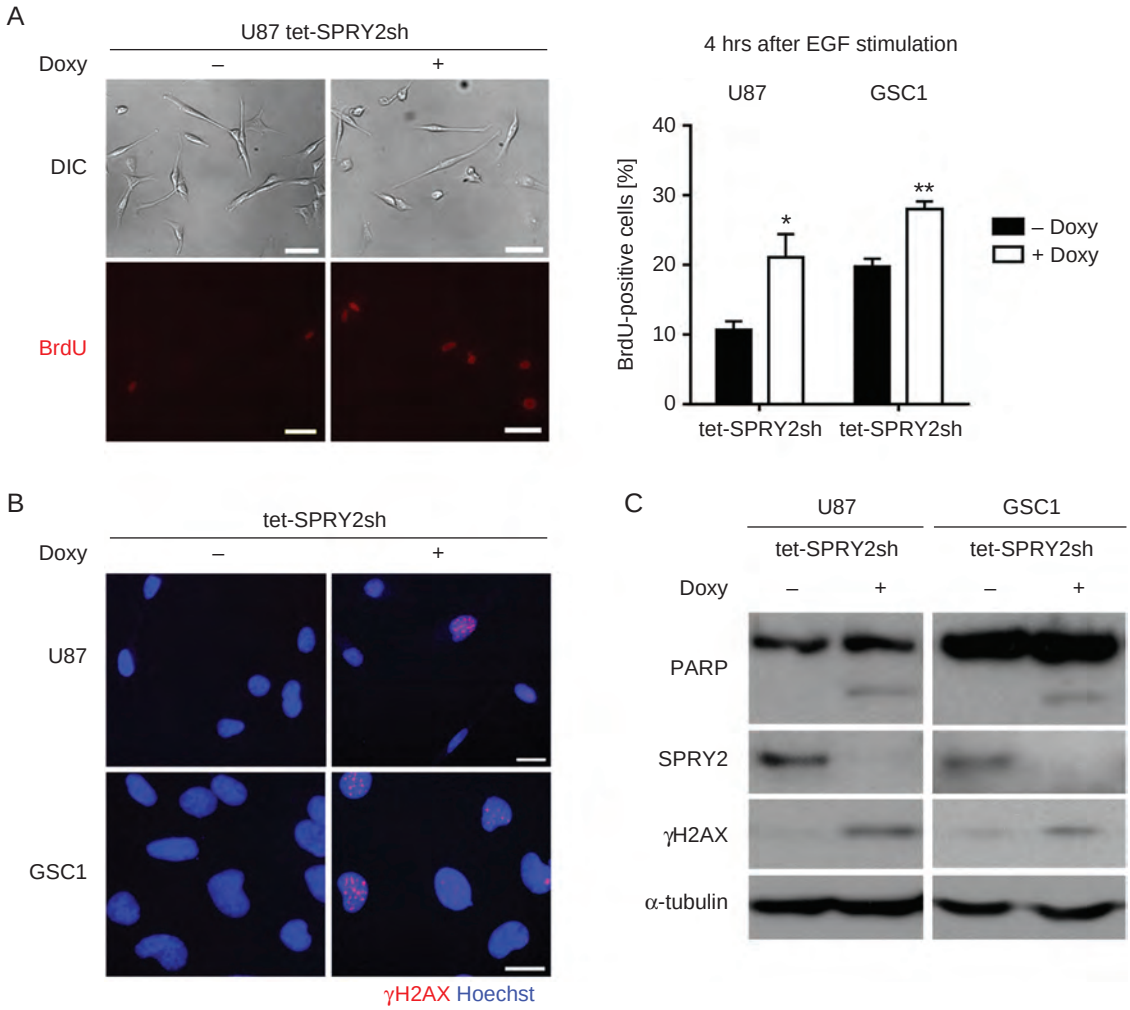

Fig. 4 Silencing of SPRY2 induces premature S-phase entry and DNA damage response. (A) Starved U87 or GSC1 tet-SPRY2sh cells (± Doxy) were stimulated with EGF for 4 hours. BrdU was added into the medium 2 hours before fixation. Representative pictures (left panel) of BrdU-positive cells in U87 tet-SPRY2sh cells (± Doxy). Scale bar = 50 μm. Quantification of BrdU-positive cells of U87 or GSC1 tet-SPRY2sh cells (± Doxy). Mean ± SEM of 3 independent experiments (right panel). $*P < 0.05$, $**P < 0.01$. Phosphorylated H2AX (B and C) and PARP cleavage (C) of U87 or GSC1 SPRY2 KD cells as determined by immunoblot or immunostaining. Scale bar = 20 μm.

B). Animal weight inversely correlated with tumor growth (Supplementary Fig. S4A). At 63 days post injection, doxycycline treatment was terminated to further examine whether a subset of tumors resides in Doxy-treated tet-SPRY2sh mice ($n = 4$). Two weeks after the termination, the tumor growth onset was observed in bioluminescence measurements (Supplementary Fig. S4B).

This pattern was also confirmed in subcutaneous xenografts. Subcutaneous tumor volumes steadily increased in Doxy-treated tet-Ctrlsh ($n = 6$) and Doxy-untreated tet-SPRY2sh mice ($n = 7$) and reached volumes of 130.1 ± 11.95 mm^3 and 136.0 ± 37.39 mm^3, respectively, at 27 days post injection (Fig. 5C, inset). Conversely, tumors derived from Doxy-treated tet-SPRY2sh mice ($n = 7$) were much smaller (32.14 ± 3.65 mm^3) (Fig. 5C, D). Doxycycline was newly administered or withdrawn in 4 out of 7 mice in tet-SPRY2sh groups at day 27, when tumor size in the Doxy-treated and -untreated groups showed significant differences (Fig. 5C, arrow). After treatment, tumors derived from the previously Doxy-untreated tet-SPRY2sh group revealed a substantial reduction in tumor size by 55% relative to control tumors over the course of the following 2 weeks (Fig. 5C). In contrast, the tumors derived from continuously Doxy-treated tet-SPRY2sh group remained viable, but without evidence of tumor growth onset for 55 days. Two weeks after removal of doxycycline, tumors grew rapidly and were larger than continuously Doxy-treated tet-SPRY2sh tumors (Fig. 5C). In Doxy-withdrawn tet-SPRY2sh tumors, the number of Ki67-positive cells was significantly increased compared with continuously Doxy-treated tet-SPRY2sh tumors (Fig. 5E).

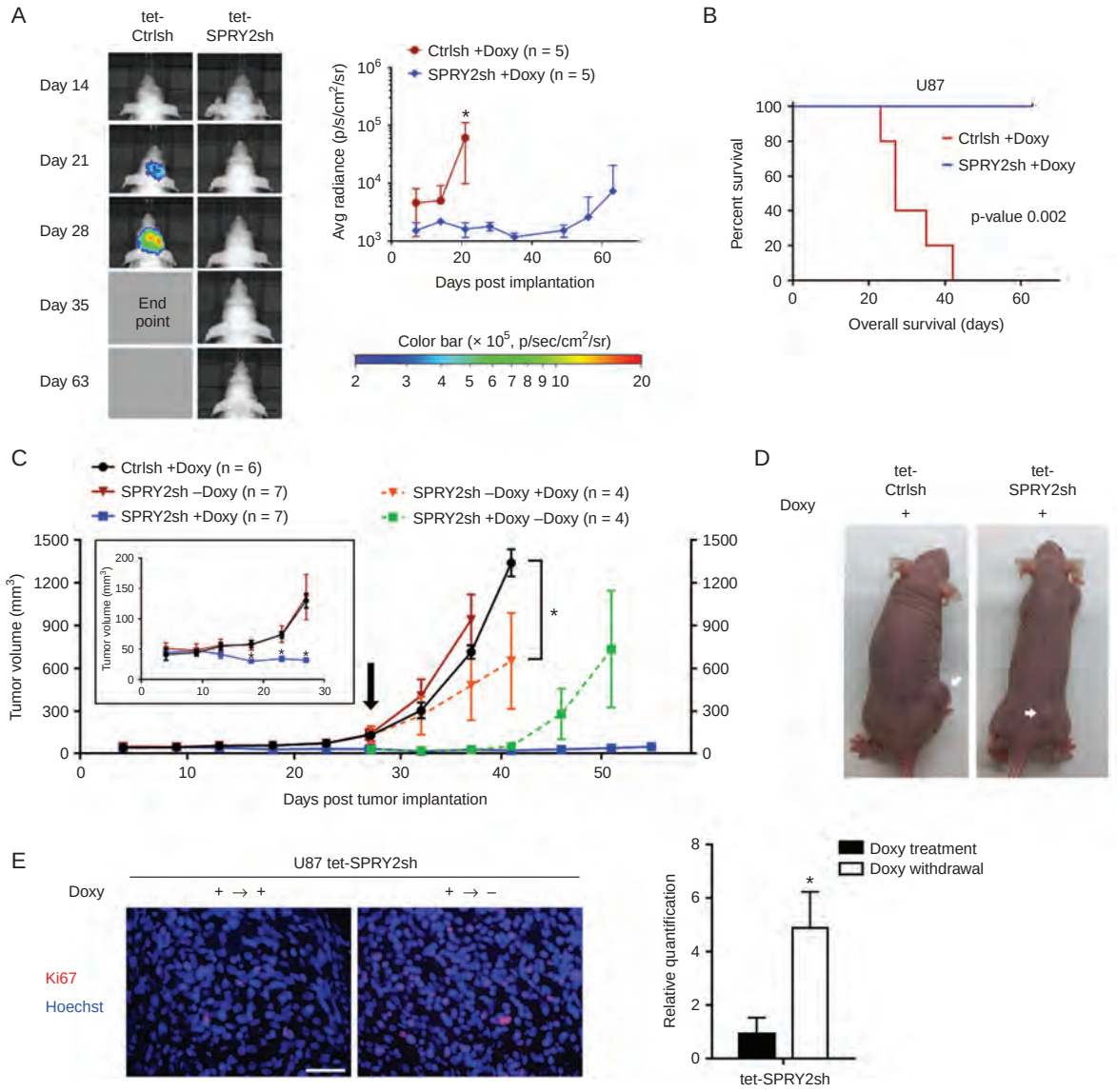

Fig. 5. Downregulation of SPRY2 inhibits U87 intracranial and subcutaneous tumor growth. (A) U87 tet-Ctrlsh or tet-SPRY2sh cells (0.5 million) expressing RNAi-resistant luciferase were intracranially injected in nude mice ($n = 5$/group) with administration of doxycycline. Representative image of bioluminescence at the indicated time point (left panel). Quantification of signal intensity presented as photons/sec/cm^2/surface radiance, *$P < 0.05$, mean ± SD (right panel). (B) Kaplan–Meier survival curve; **$P < 0.01$ by the log-rank test. (C) U87 tet-Ctrlsh or tet-SPRY2sh cells (2 million) were subcutaneously injected in nude mice ($n = 6$–7/group) with or without administration of doxycycline. Early stage of subcutaneous tumor development is displayed (inset). Later tumor development following doxycycline treatment in 4 out of 7 previously doxy-untreated tet-SPRY2sh tumor-bearing mice is highlighted in orange. Tumor growth after doxycycline withdrawal in 4 out of 7 doxy-treated tet-SPRY2sh tumor-bearing mice is highlighted in green. *$P < 0.05$, mean ± SD. (D) Representative pictures of tet-Ctrlsh or tet-SPRY2sh tumor-bearing mice (+Doxy) are shown (arrows indicate tumor). Scale bar = 50 μm. (E) Representative images and quantification of Ki67-positive cells in U87 tet-SPRY2sh tissues (± Doxy). *$P < 0.05$.

SPRY2 Overexpression Promotes Tumor Propagation of Low-Tumorigenic U251 Cells

To further examine the effect of SPRY2 on GBM tumor growth, we utilized U251 cells, which express very low levels of endogenous SPRY2, making them a suitable cell line for overexpression (OE) experiments (Fig. 6A). As phosphorylation of serine 121 was shown to be important for the functionality of SPRY2,[33] we also generated U251 cells expressing a SPRY2^{S121A} mutant using lentiviral gene expression vectors (Fig. 6A). As a control for lentiviral gene expression, we transduced U251 cells with a lentiviral construct expressing VNP (Venus-NLS-PEST) fluorescent protein. Proliferation capacity and cell cycle progression was

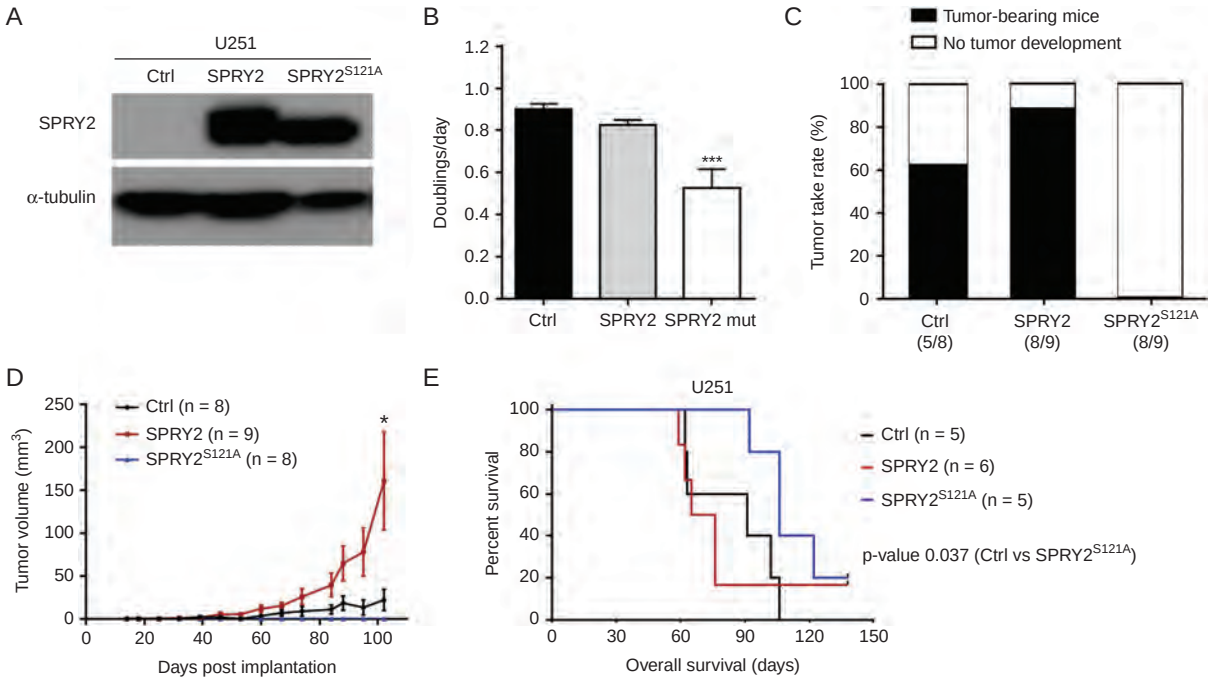

Fig. 6 SPRY2 overexpression enhances U251 tumor growth and reduces survival of mice. (A) SPRY2 protein levels of U251 cells transduced with Ctrl (VNP), SPRY2, or SPRY2^{S121A} are shown using immunoblot. (B) Doublings per day of U251 expressing Ctrl, SPRY2, or SPRY2^{S121A} as assessed by cell counting. ***$P < 0.001$, mean ± SEM. (C) Mice ($n = 8$–9/group) were injected subcutaneously with U251 Ctrl, SPRY2, or SPRY2^{S121A} cells (1.5 million). The tumorigenic capacity was assessed as the percentage of tumor take rate. (D) The size of subcutaneous tumor xenografts following weekly measurements. *$P < 0.05$, mean ± SD. (E) U251 Ctrl, SPRY2, or SPRY2^{S121A} cells (1 million) were intracranially injected in nude mice ($n = 5$–6/group). Kaplan–Meier survival curve; *$P < 0.05$ Ctrl vs SPRY2^{S121A} by the log-rank test.

comparable between U251 Ctrl and SPRY2 OE cells (Fig. 6B and Supplementary Fig. S5A, B), but SPRY2^{S121A} mutant OE inhibited cell proliferation of U251 cells (Fig. 6B).

To test the effect of SPRY2 on U251 xenografts, U251 cells expressing VNP (Ctrl, $n = 8$), SPRY2 ($n = 9$), or SPRY2^{S121A} ($n = 8$) were subcutaneously injected into nude mice. As a result, U251 SPRY2 OE mice exhibited a 26% increase in tumor take rate compared with U251 Ctrl, while there was no tumor formation in the SPRY2 serine mutant (S121A) OE mice (Fig. 6C). U251 SPRY2 OE subcutaneous tumors were 7 times larger by volume compared with Ctrl at 102 days post injection (Fig. 6D). Similarly, the survival of orthotopic xenografted mice was reduced in the case of U251 SPRY2 OE transplants (median 70.5 days) compared with controls (median 91 days), while survival was significantly increased in mice transplanted with SPRY2^{S121A} OE cells (median 106 days) ($P = 0.037$; Fig. 6E).

Discussion

SPRY2 expression in GBM is higher than that in lower-grade glioma and nontumor tissues. Among the established GBM cell lines, U87 cells strongly express SPRY2, whereas U251 and T98G cells express low levels of SPRY2. U87 cells are a widely used cell line for tumor xenograft models, as they have a high tumorigenic potential in mice. In contrast, U251 and T98G cells are known to be less tumorigenic, implying that there might be a correlation between SPRY2 expression and tumorigenic capacity. Further supporting this hypothesis, the Kaplan–Meier plot indicates that GBM patients with low expression of *SPRY2* had significantly prolonged survival.

Cell proliferation is significantly impaired by shRNA-mediated downregulation of SPRY2 in GBM cells. Our study showed that SPRY2 KD decreases cell proliferation with the concomitant increase of ERK and Akt activation. In contrast, inhibiting MEK activity restored proliferation of SPRY2 KD cells, indicating that the reduced proliferation upon SPRY2 KD is a consequence of excessive ERK signaling, and antiproliferative efficacy of MEK inhibitor depends on the strength of ERK activation. This is consistent with previous findings that suppression of ERK levels or activity in both human and mouse primary cells prevented proliferation arrest due to oncogenic stress induced by activated Ras.[34] Zhang et al[35] also reported that SPRY2 KD decreases cell proliferation of colon cancer cells in the presence of increased EGF-dependent ERK and Akt signaling and induction of the cyclin-dependent kinase inhibitor p21^{CIP1}. We suggest here that decreased cell proliferation may be caused by oncogene-induced DNA replication stress because silencing SPRY2 causes premature S-phase entry and increased DNA damage. In parallel with these findings,

our data revealed that cytotoxicity and PARP cleavage are increased upon SPRY2 suppression. Thus, the canonical function of SPRY2 (ie, in dampening the MAPK pathway) appears to be required for proliferation and normal DNA replication by limiting oncogenic stress in primary GBM cells as well as established GBM cell lines.

It has been proposed that DNA replication stress can be exploited for cancer therapy because it is rarely detected in normal cells.[32] Consistent with this, our study showed that the proliferation capacity of normal astrocytes is not attenuated by SPRY2 inhibition. Additionally, given that the expression of SPRY2 in normal tissues is significantly lower than in GBM tissues, nontumoral cells are unlikely targets for SPRY2 suppression.

Silencing of SPRY2 in cells grown in culture slowed down proliferation in part by inducing cell death. These effects were even more dramatic in vivo as knockdown of SPRY2 prevented tumor growth over the observation period of 9 weeks. Immunohistochemical analysis of Ki67 showed that the strong inhibitory effect on tumor propagation is likely due to proliferation arrest in response to SPRY2 suppression. After doxycycline termination at day 63, tumor growth resumed with similar kinetics to control tumors. Similar results were obtained in heterotopic tumor transplantation experiments, demonstrating that SPRY2 depletion by RNAi in vivo was not sufficient to eradicate tumor cells but more likely induced a reversible growth arrest, whose dormancy required continuous administration of doxycycline to downregulate SPRY2 expression.

Consistent with the hypothesis that SPRY2 is required for efficient tumor formation, SPRY2 OE enhanced tumor growth and reduced survival of tumor cells in xenotransplanted mice. As expected, ERK activity in U251 SPRY2 OE cells was decreased (data not shown), but this did not impact on proliferation in vitro. The strong tumor-promoting effect of SPRY2 OE in vivo most likely thus depends on additional factors such as tumor microenvironment or growth conditions in vivo compared with in vitro. The underlying mechanism for this effect needs to be addressed in future studies. Surprisingly, however, the SPRY2 serine mutant (S121A) OE strongly inhibited cell proliferation in culture and subcutaneous tumor growth. In line with this, the survival of mice was prolonged in mice intracranially implanted with U251 cells expressing mutants versus wild-type SPRY2 or control cells expressing VNP. That overexpression of SPRY2 (S121A) blocks proliferation and delays tumor formation in vivo was unexpected but may be due to a dominant negative effect, highlighting the potential of SPRY2 manipulation for tumor therapy.

We postulate that SPRY2 is important for cell proliferation and tumorigenicity in a subset of GBM. Targeting SPRY2 causes excessive ERK activation and sensitizes GBM cells to DNA damage response that eventually leads to decreased proliferation and reduced tumorigenic capacity. The results of this study may provide a molecular basis for novel therapeutic strategies targeting GBM.

Supplementary Material

Supplementary material is available at *Neuro-Oncology* online.

Funding

This study was supported by the Austrian Science Fund (FWF, W 1206-B18) and the Christian Doppler Research Association.

Acknowledgments

We would like to thank Markus Reindl for providing established GBM cell lines. We are grateful to Ana Curinha for helping out with FACS analyses.

Conflict of interest statement. The authors declare no conflicts of interest.

References

1. Louis DN, Ohgaki H, Wiestler OD, et al. The 2007 WHO classification of tumours of the central nervous system. *Acta Neuropathol*. 2007;114(2):97–109.
2. Stupp R, Mason WP, van den Bent MJ, et al; European Organisation for Research and Treatment of Cancer Brain Tumor and Radiotherapy Groups; National Cancer Institute of Canada Clinical Trials Group. Radiotherapy plus concomitant and adjuvant temozolomide for glioblastoma. *N Engl J Med*. 2005;352(10):987–996.
3. Furnari FB, Fenton T, Bachoo RM, et al. Malignant astrocytic glioma: genetics, biology, and paths to treatment. *Genes Dev*. 2007;21(21):2683–2710.
4. Patel AP, Tirosh I, Trombetta JJ, et al. Single-cell RNA-seq highlights intratumoral heterogeneity in primary glioblastoma. *Science*. 2014;344(6190):1396–1401.
5. Cancer Genome Atlas Research Network. Comprehensive genomic characterization defines human glioblastoma genes and core pathways. *Nature*. 2008;455(7216):1061–1068.
6. Hacohen N, Kramer S, Sutherland D, Hiromi Y, Krasnow MA. sprouty encodes a novel antagonist of FGF signaling that patterns apical branching of the Drosophila airways. *Cell*. 1998;92(2):253–263.
7. Casci T, Vinós J, Freeman M. Sprouty, an intracellular inhibitor of Ras signaling. *Cell*. 1999;96(5):655–665.
8. Minowada G, Jarvis LA, Chi CL, et al. Vertebrate Sprouty genes are induced by FGF signaling and can cause chondrodysplasia when overexpressed. *Development*. 1999;126(20):4465–4475.
9. Masoumi-Moghaddam S, Amini A, Morris DL. The developing story of Sprouty and cancer. *Cancer Metastasis Rev*. 2014;33(2-3):695–720.
10. Lo TL, Yusoff P, Fong CW, et al. The ras/mitogen-activated protein kinase pathway inhibitor and likely tumor suppressor proteins, sprouty 1 and sprouty 2 are deregulated in breast cancer. *Cancer Res*. 2004;64(17):6127–6136.
11. Fong CW, Chua MS, McKie AB, et al. Sprouty 2, an inhibitor of mitogen-activated protein kinase signaling, is down-regulated in hepatocellular carcinoma. *Cancer Res*. 2006;66(4):2048–2058.
12. Sutterlüty H, Mayer CE, Setinek U, et al. Down-regulation of Sprouty2 in non-small cell lung cancer contributes to tumor malignancy via

extracellular signal-regulated kinase pathway-dependent and -independent mechanisms. *Mol Cancer Res*. 2007;5(5):509–520.
13. McKie AB, Douglas DA, Olijslagers S, et al. Epigenetic inactivation of the human sprouty2 (hSPRY2) homologue in prostate cancer. *Oncogene*. 2005;24(13):2166–2174.
14. Barbáchano A, Ordóñez-Morán P, García JM, et al. SPROUTY-2 and E-cadherin regulate reciprocally and dictate colon cancer cell tumourigenicity. *Oncogene*. 2010;29(34):4800–4813.
15. Holgren C, Dougherty U, Edwin F, et al. Sprouty-2 controls c-Met expression and metastatic potential of colon cancer cells: sprouty/c-Met upregulation in human colonic adenocarcinomas. *Oncogene*. 2010;29(38):5241–5253.
16. Kwak HJ, Kim YJ, Chun KR, et al. Downregulation of Spry2 by miR-21 triggers malignancy in human gliomas. *Oncogene*. 2011;30(21):2433–2442.
17. Walsh AM, Kapoor GS, Buonato JM, et al. Sprouty2 drives drug resistance and proliferation in glioblastoma. *Mol Cancer Res*. 2015;13(8):1227–1237.
18. Zhang W, Lv Y, Xue Y, et al. Co-expression modules of NF1, PTEN and sprouty enable distinction of adult diffuse gliomas according to pathway activities of receptor tyrosine kinases. *Oncotarget*. 2016;7(37):59098–59114.
19. Corsaro A, Bajetto A, Thellung S, et al. Cellular prion protein controls stem cell-like properties of human glioblastoma tumor-initiating cells. *Oncotarget*. 2016;7(25):38638–38657.
20. Sigl R, Ploner C, Shivalingaiah G, Kofler R, Geley S. Development of a multipurpose GATEWAY-based lentiviral tetracycline-regulated conditional RNAi system (GLTR). *PLoS One*. 2014;9(5):e97764.
21. Rathmanner N, Haigl B, Vanas V, Doriguzzi A, Gsur A, Sutterlüty-Fall H. Sprouty2 but not Sprouty4 is a potent inhibitor of cell proliferation and migration of osteosarcoma cells. *FEBS Lett*. 2013;587(16):2597–2605.
22. Dold C, Rodriguez Urbiola C, Wollmann G, et al. Application of interferon modulators to overcome partial resistance of human ovarian cancers to VSV-GP oncolytic viral therapy. *Mol Ther Oncolytics*. 2016;3:16021.
23. Murat A, Migliavacca E, Gorlia T, et al. Stem cell-related "self-renewal" signature and high epidermal growth factor receptor expression associated with resistance to concomitant chemoradiotherapy in glioblastoma. *J Clin Oncol*. 2008;26(18):3015–3024.
24. Sturm D, Witt H, Hovestadt V, et al. Hotspot mutations in H3F3A and IDH1 define distinct epigenetic and biological subgroups of glioblastoma. *Cancer Cell*. 2012;22(4):425–437.
25. Sun L, Hui AM, Su Q, et al. Neuronal and glioma-derived stem cell factor induces angiogenesis within the brain. *Cancer Cell*. 2006;9(4):287–300.
26. Rhodes DR, Yu J, Shanker K, et al. ONCOMINE: a cancer microarray database and integrated data-mining platform. *Neoplasia*. 2004;6(1):1–6.
27. Bowman RL, Wang Q, Carro A, Verhaak RG, Squatrito M. GlioVis data portal for visualization and analysis of brain tumor expression datasets. *Neuro Oncol*. 2017;19(1):139–141.
28. Ceccarelli M, Barthel FP, Malta TM, et al; TCGA Research Network. Molecular profiling reveals biologically discrete subsets and pathways of progression in diffuse glioma. *Cell*. 2016;164(3):550–563.
29. Lee J, Kotliarova S, Kotliarov Y, et al. Tumor stem cells derived from glioblastomas cultured in bFGF and EGF more closely mirror the phenotype and genotype of primary tumors than do serum-cultured cell lines. *Cancer Cell*. 2006;9(5):391–403.
30. Gross I, Bassit B, Benezra M, Licht JD. Mammalian sprouty proteins inhibit cell growth and differentiation by preventing ras activation. *J Biol Chem*. 2001;276(49):46460–46468.
31. Gao M, Patel R, Ahmad I, et al. SPRY2 loss enhances ErbB trafficking and PI3K/AKT signalling to drive human and mouse prostate carcinogenesis. *EMBO Mol Med*. 2012;4(8):776–790.
32. Gaillard H, García-Muse T, Aguilera A. Replication stress and cancer. *Nat Rev Cancer*. 2015;15(5):276–289.
33. DaSilva J, Xu L, Kim HJ, Miller WT, Bar-Sagi D. Regulation of sprouty stability by Mnk1-dependent phosphorylation. *Mol Cell Biol*. 2006;26(5):1898–1907.
34. Deschênes-Simard X, Gaumont-Leclerc MF, Bourdeau V, et al. Tumor suppressor activity of the ERK/MAPK pathway by promoting selective protein degradation. *Genes Dev*. 2013;27(8):900–915.
35. Zhang Q, Shim K, Wright K, Jurkevich A, Khare S. Atypical role of sprouty in p21 dependent inhibition of cell proliferation in colorectal cancer. *Mol Carcinog*. 2016;55(9):1355–1368.